

**Science**

 AAAS

**Live-Cell Imaging of Enzyme-Substrate Interaction  
Reveals Spatial Regulation of PTP1B**

Ivan A. Yudushkin, *et al.*  
*Science* **315**, 115 (2007);  
DOI: 10.1126/science.1134966

**The following resources related to this article are available online at  
[www.sciencemag.org](http://www.sciencemag.org) (this information is current as of January 10, 2008 ):**

**Updated information and services**, including high-resolution figures, can be found in the online version of this article at:

<http://www.sciencemag.org/cgi/content/full/315/5808/115>

**Supporting Online Material** can be found at:

<http://www.sciencemag.org/cgi/content/full/315/5808/115/DC1>

A list of selected additional articles on the Science Web sites **related to this article** can be found at:

<http://www.sciencemag.org/cgi/content/full/315/5808/115#related-content>

This article **cites 22 articles**, 9 of which can be accessed for free:

<http://www.sciencemag.org/cgi/content/full/315/5808/115#otherarticles>

This article has been **cited by** 4 article(s) on the ISI Web of Science.

This article has been **cited by** 2 articles hosted by HighWire Press; see:

<http://www.sciencemag.org/cgi/content/full/315/5808/115#otherarticles>

This article appears in the following **subject collections**:

Cell Biology

[http://www.sciencemag.org/cgi/collection/cell\\_biol](http://www.sciencemag.org/cgi/collection/cell_biol)

Information about obtaining **reprints** of this article or about obtaining **permission to reproduce this article** in whole or in part can be found at:

<http://www.sciencemag.org/about/permissions.dtl>

their time bound to moving F-actin and part of their time bound to a less mobile FA component, thus identifying these proteins as a site of slippage in the F-actin/FA interface. Alternatively, differential coupling of FA proteins to transverse actin bundles and stress fibers in the lamella could contribute to the observed effect. However, given the local slowing of F-actin flow in the FA in the lamella and the biophysical evidence implicating talin and vinculin in force transmission in the FA (20, 25, 26), we suspect that these proteins form transient linkages across the slippage interface, resulting in force-transducing slip-stick friction between F-actin and the ECM. The degree of molecular motion transmission through the FA was regulated, and it was correlated with protrusion and retraction events during cell migration. Therefore, FA internal molecular kinematics may be a key element in the integrin-mediated translation of intracellular biochemistry into cellular mechanics during cell and tissue morphogenesis, or in the reception of extracellular mechanical signals to mediate sensory perception, tissue maintenance, and differentiation (27).

#### References and Notes

1. D. A. Lauffenburger, A. F. Horwitz, *Cell* **84**, 359 (1996).

2. K. Burridge, M. Chrzanoska-Wodnicka, *Annu. Rev. Cell Dev. Biol.* **12**, 463 (1996).
3. C. H. Lin, P. Forscher, *Neuron* **14**, 763 (1995).
4. B. Geiger, A. Bershadsky, R. Pankov, K. M. Yamada, *Nat. Rev. Mol. Cell Biol.* **2**, 793 (2001).
5. R. J. Pelham Jr., Y. Wang, *Proc. Natl. Acad. Sci. U.S.A.* **94**, 13661 (1997).
6. K. Maruyama, S. Ebashi, *J. Biochem. (Tokyo)* **58**, 13 (1965).
7. M. Muguruma, S. Matsumura, T. Fukazawa, *Biochem. Biophys. Res. Commun.* **171**, 1217 (1990).
8. R. P. Johnson, S. W. Craig, *Nature* **373**, 261 (1995).
9. T. Tanaka, R. Yamaguchi, H. Sabe, K. Sekiguchi, J. M. Healy, *FEBS Lett.* **399**, 53 (1996).
10. D. A. Calderwood *et al.*, *J. Biol. Chem.* **274**, 28071 (1999).
11. K. Burridge, P. Mangeat, *Nature* **308**, 744 (1984).
12. M. C. Beckerle, *Bioessays* **19**, 949 (1997).
13. D. D. Schlaepfer, T. Hunter, *Cell Struct. Funct.* **21**, 445 (1996).
14. K. M. Yamada, S. Miyamoto, *Curr. Opin. Cell Biol.* **7**, 681 (1995).
15. M. Chrzanoska-Wodnicka, K. Burridge, *J. Cell Biol.* **133**, 1403 (1996).
16. A. Ponti, M. Machacek, S. L. Gupton, C. M. Waterman-Storer, G. Danuser, *Science* **305**, 1782 (2004).
17. L. Ji, G. Danuser, *J. Microsc.* **220**, 150 (2005).
18. Materials and methods are available as supporting material on Science Online.
19. B. Geiger, *Cell* **18**, 193 (1979).
20. G. Jiang, G. Giannone, D. R. Critchley, E. Fukumoto, M. P. Sheetz, *Nature* **424**, 334 (2003).
21. C. E. Turner, J. R. Glenney Jr., K. Burridge, *J. Cell Biol.* **111**, 1059 (1990).
22. S. L. Gupton *et al.*, *J. Cell Biol.* **168**, 619 (2005).
23. M. Edlund, M. A. Lotano, C. A. Otey, *Cell Motil. Cytoskelet.* **48**, 190 (2001).
24. G. Giannone *et al.*, *Cell* **116**, 431 (2004).
25. R. M. Ezzell, W. H. Goldmann, N. Wang, N. Parasharama, D. E. Ingber, *Exp. Cell Res.* **231**, 14 (1997).
26. G. Giannone, G. Jiang, D. H. Sutton, D. R. Critchley, M. P. Sheetz, *J. Cell Biol.* **163**, 409 (2003).
27. A. Katsumi, A. W. Orr, E. Tzima, M. A. Schwartz, *J. Biol. Chem.* **279**, 12001 (2004).
28. We thank C. Otey (University of North Carolina, Chapel Hill), A. Huttenlocher (University of Wisconsin, Madison), D. Schlaepfer (Scripps), A. F. Horwitz (University of Virginia, Charlottesville), I. Kaverina (Vanderbilt University), and M. Ginsberg (University of California, San Diego) for complementary DNAs. Supported by NIH grants GM67230 (C.M.W.-S. and G.D.) and U54GM64346 (G.D. and L.J.), American Heart Association Established Investigatorship and NIH Director's Pioneer Award (C.M.W.-S.), Leukemia and Lymphoma Society (K.H.), and NSF (K.T.A.).

#### Supporting Online Material

www.sciencemag.org/cgi/content/full/315/5808/111/DC1  
Materials and Methods

Figs. S1 to S8

Tables S1 to S5

References

Movies S1 to S14

13 September 2006; accepted 16 November 2006

10.1126/science.1135085

# Live-Cell Imaging of Enzyme-Substrate Interaction Reveals Spatial Regulation of PTP1B

Ivan A. Yudushkin,<sup>1\*</sup> Andreas Schleifenbaum,<sup>1\*</sup> Ali Kinkhabwala,<sup>1\*</sup> Benjamin G. Neel,<sup>2</sup> Carsten Schultz,<sup>1</sup> Philippe I. H. Bastiaens<sup>1†</sup>

Endoplasmic reticulum-localized protein-tyrosine phosphatase PTP1B terminates growth factor signal transduction by dephosphorylation of receptor tyrosine kinases (RTKs). But how PTP1B allows for RTK signaling in the cytoplasm is unclear. In order to test whether PTP1B activity is spatially regulated, we developed a method based on Förster resonant energy transfer for imaging enzyme-substrate (ES) intermediates in live cells. We observed the establishment of a steady-state ES gradient across the cell. This gradient exhibited robustness to cell-to-cell variability, growth factor activation, and RTK localization, which demonstrated spatial regulation of PTP1B activity. Such regulation may be important for generating distinct cellular environments that permit RTK signal transduction and that mediate its eventual termination.

Protein-tyrosine phosphorylation is widely used by eukaryotic cells to transduce signals, but the dynamic interplay between receptor tyrosine kinases (RTKs) and protein-tyrosine

phosphatases (PTPs) remains poorly understood (1, 2). The protein tyrosine phosphatase-1B (PTP1B) resides on the surface of the endoplasmic reticulum (ER) (3, 4) and helps terminate signaling by multiple RTKs, including the epidermal growth factor receptor (EGFR) (5). Previous reports demonstrate that RTK signaling occurs at the plasma membrane and endosomes (6), and its termination occurs along the ER surface (7–11). Because PTP1B has much higher specific activity than typical RTKs in vitro (12, 13), uniformly high PTP1B activity along the ER could prevent endosomal RTK signaling. To

account for compartmentalized RTK signaling, we hypothesized that PTP1B might exist inside cells as spatially separated subpopulations with different kinetic properties.

To test this hypothesis, we developed an imaging approach based on Förster resonant energy transfer (FRET) to spatially resolve enzyme-substrate (ES) interactions and thereby to monitor enzyme activity in live cells (Fig. 1A) (11). We tagged PTP1B with a donor chromophore by fusion to a genetically encoded fluorescent protein, and conjugated the substrate, a synthetic phosphotyrosine-containing peptide, to an acceptor chromophore (Fig. 1B). For Michaelis-Menten kinetics, the steady-state fraction ( $\alpha$ ) of ES complex to total enzyme ( $E_0$ ) is as follows:

$$\alpha = ES/E_0 = S/(K_M + S) \quad (1)$$

where  $S$  is the substrate concentration, and  $K_M$  is the Michaelis-Menten constant. The fraction  $\alpha$  can be mapped across the cell by quantitatively imaging FRET with the use of fluorescence lifetime imaging microscopy (FLIM) (14–16).

We first tested whether formation of the ES intermediate could be detected by FRET in vitro. To stabilize the ordinarily transient ES intermediate and thereby to facilitate FRET detection, we used the purified enhanced green fluorescent protein (EGFP)-tagged catalytically impaired mutant of PTP1B that retains substrate-binding ability (residues 1 to 321, PTP1B<sup>D181A</sup>, in which Ala<sup>181</sup> was substituted for Asp) (17, 18). Indeed, FRET in the ES complex was apparent, as in-

<sup>1</sup>European Molecular Biology Laboratory (EMBL), Meyerhofstrasse 1, D-69117 Heidelberg, Germany. <sup>2</sup>Cancer Biology Program, Division of Hematology-Oncology, Department of Medicine, Beth Israel Deaconess Medical Center, Harvard Medical School, 77 Avenue Louis Pasteur, Boston, MA 02115, USA.

\*These authors contributed equally to this work.

†To whom correspondence should be addressed. E-mail: bastiaens@embl.de

indicated by increased acceptor (lissamine) emission, quenching of donor (EGFP) fluorescence (Fig. 1C), and decreased donor fluorescence lifetime (fig. S3). Consistent with the PTP catalytic mechanism, the thiol-reactive compounds iodoacetamide and sodium pervanadate (19), as well as the transition-state analog sodium vanadate, all attenuated FRET (Fig. 1D and fig. S3). By contrast, incubation of the peptide with the wild-type catalytic domain resulted in a transient FRET signal, which decayed with a velocity consistent with previously determined catalytic parameters [ $K_M$  of 2.2  $\mu\text{M}$ , and the catalytic rate of the enzyme ( $k_{\text{cat}}$ ) of 67  $\text{s}^{-1}$ ; fig. S4] (13, 20).

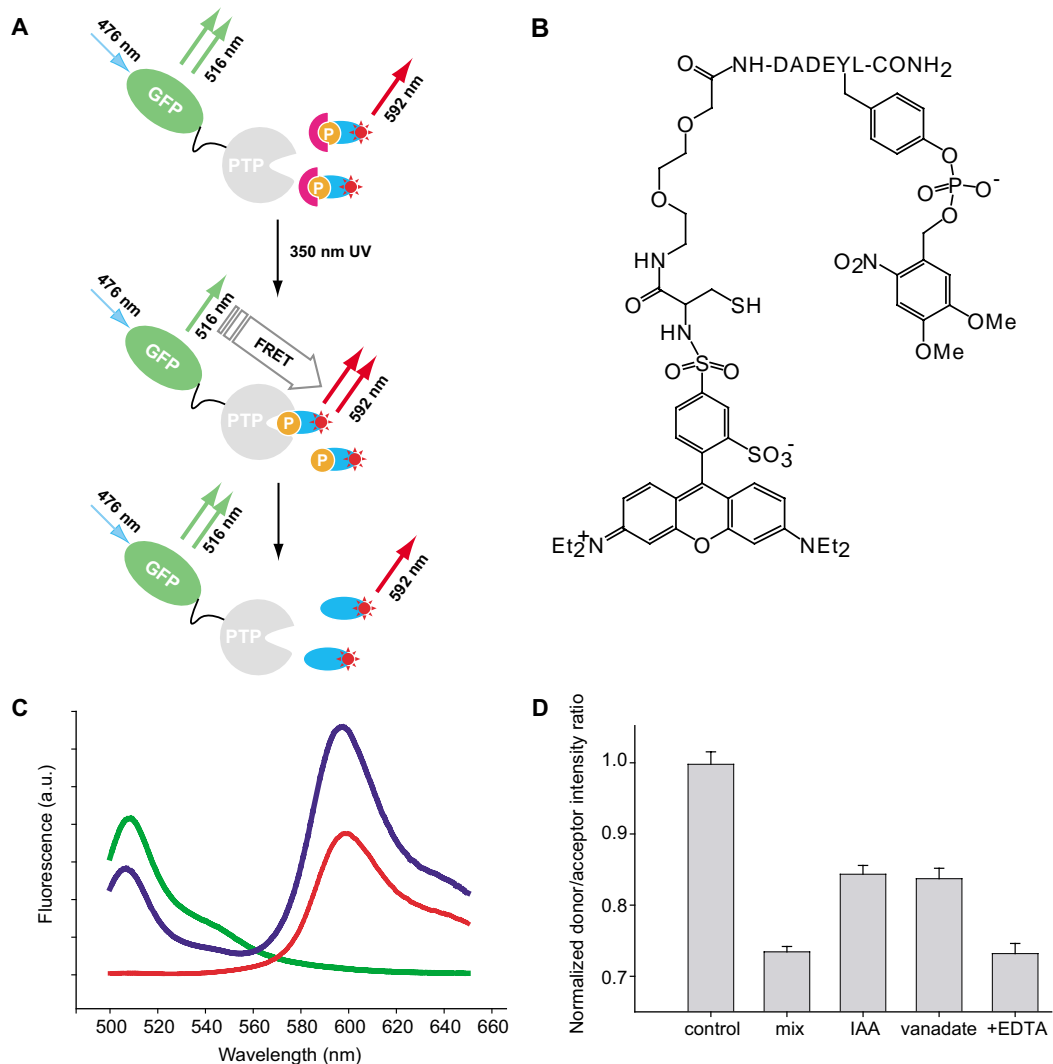
Next, we analyzed interactions between PTP1B and the synthetic substrate in COS-7 cells, which endogenously express EGFR (21). We compared the EGFP fluorescence lifetime in cells ectopically expressing EGFP-PTP1B<sup>WT</sup> with and without microinjected caged substrate (1-cP) (Fig. 2A). As expected, no FRET signal

was observed before uncaging, because the cage on the phosphate moiety prevents ES interaction (22) (Fig. 2B, top). Ultraviolet (UV)-induced uncaging resulted in a significant drop of EGFP fluorescence lifetime, only in substrate-injected cells (Fig. 2B, middle), indicative of FRET. This interaction was specific for the phosphorylated peptide, as no FRET was detected when EGFR-deficient MCF-7 cells were loaded with the cognate nonphosphorylated peptide (see below). A transient, uniform distribution of ES complex was observed 15 s after uncaging, which evolved to a persistent gradient of ES complex by 1 min (Fig. 2C), with higher ES complex at the cell periphery. This slow equilibration time scale is inconsistent with the high  $k_{\text{cat}}$  measured in vitro (67  $\mu\text{M s}^{-1}$  turnover for 1  $\mu\text{M}$  of ES complex), which suggests that  $k_{\text{cat}}$  in vivo is <1% of that in vitro and/or only a small fraction (<1%) of PTP1B is fully active in vivo. The expected rapid equilibration time scale of <1 s was more rigorously confirmed by analysis of the time domain of

a reaction-diffusion model (discussed below) that assumes the in vitro kinetic parameters.

The establishment of a stable ES complex concentration after stepwise uncaging of the substrate in COS-7 cells implied a steady-state maintained by a phosphorylation-dephosphorylation cycle (Fig. 2E). Notably, peptides containing the DADEYL phosphorylation motif can bind and be phosphorylated by the high basal kinase activity of the EGFR in the absence of epidermal growth factor (EGF) (12, 18, 23). To verify that ES complex was maintained at a steady state by a kinase-phosphatase reaction cycle, we tested whether nonphosphorylated substrate could be phosphorylated in cells. Loading a membrane-permeant, nonphosphorylated analog of the substrate (peptide 2-OH) into MCF-7 cells ectopically coexpressing the citrine variant of yellow fluorescent protein fused to PTP1B<sup>D181A</sup> (citrine-PTP1B<sup>D181A</sup>) and cyan fluorescent protein fused to EGFR<sup>WT</sup> (EGFR<sup>WT</sup>-CFP) resulted in accumulation of substrate-PTP1B<sup>D181A</sup> complex over

**Fig. 1. Monitoring ES intermediate by FRET. (A)** Assay format. (Top) A photolabile chemical protection group ("cage") on the phosphate moiety of the phosphotyrosine-containing synthetic peptide prevents binding to the active site of the PTP. (Middle) UV-induced photolysis of the cage induces substrate binding at the PTP active site and FRET, monitored by FLIM and/or emission intensity changes. (Bottom) After catalysis, the reaction product dissociates from the PTP, resulting in loss of FRET. **(B)** The synthetic hexapeptide substrate (LRh-Cys-AEEAc-DADEY<sup>NVOP</sup>L-CONH<sub>2</sub>, 2-cP), corresponding to amino acids 988 to 993 of EGFR (phosphorylation at Y992), contains a photolabile 6-nitroveratryloxyphosphoryl (NVOP) group on the tyrosine residue and is coupled with FRET acceptor fluorophore lissamine rhodamine B (LRh) via an amino-ethoxy-ethoxy-acetyl (AEEAc) linker. An alternative peptide (1-cP) with an aminohexanoic (Ahx) acid linker and lacking the cysteine is not shown. For some live-cell experiments, 2-cP was coupled to the cell internalization sequence from the third helix of the Antennapedia homeodomain (26). **(C)** Stabilization of the ES intermediate causes FRET between the EGFP-PTP1B(1–321)<sup>D181A</sup> (green) and LRh-Ahx-DADEY<sup>P</sup>L-CONH<sub>2</sub> (red) as seen by decreased emission of EGFP and increased fluorescence of lissamine on excitation at 476 nm (blue trace). **(D)** The thiol-reactive compound iodoacetamide (IAA) or the transition-state analog vanadate inhibits formation of the ES complex in vitro. EDTA chelates vanadate, reversing competitive inhibition of the substrate binding to EGFP-PTP1B(1–321)<sup>D181A</sup>. Error bars show the SD of a typical experiment ( $n = 3$ ).



time. This complex was not observed in the absence of EGFR<sup>WT</sup> or when the kinase-dead mutant EGFR<sup>V741G</sup> was transfected (Fig. 2F). Irreversible PTP inhibitor sodium pervanadate or the specific EGFR kinase inhibitor gefitinib (Iressa) also decreased FRET between citrine-tagged PTP1B and the substrate (figs. S7 and S8) in EGFR<sup>WT</sup>-expressing MCF-7 cells, which confirmed the dynamics of the reaction cycle.

Because this reaction cycle establishes a steady-state concentration of the phosphorylated substrate, we could analyze the spatial distribution of ES complexes. Notably, the steady-state concentration of the ES complex was higher at the cell periphery than in the perinuclear region (Fig. 3, A to C). Using Eq. 1, a map of  $K_M/S$  for PTP1B<sup>WT</sup> was constructed (Fig. 3D), which revealed that the peripheral pool of PTP1B operated in a near-saturation regime (i.e., low  $K_M/S$ ). An ES gradient dependent on  $K_M$  and  $S$  could reflect spatial regulation of PTP1B catalytic activity (by its effect on  $K_M$ ). Alternatively, such a gradient

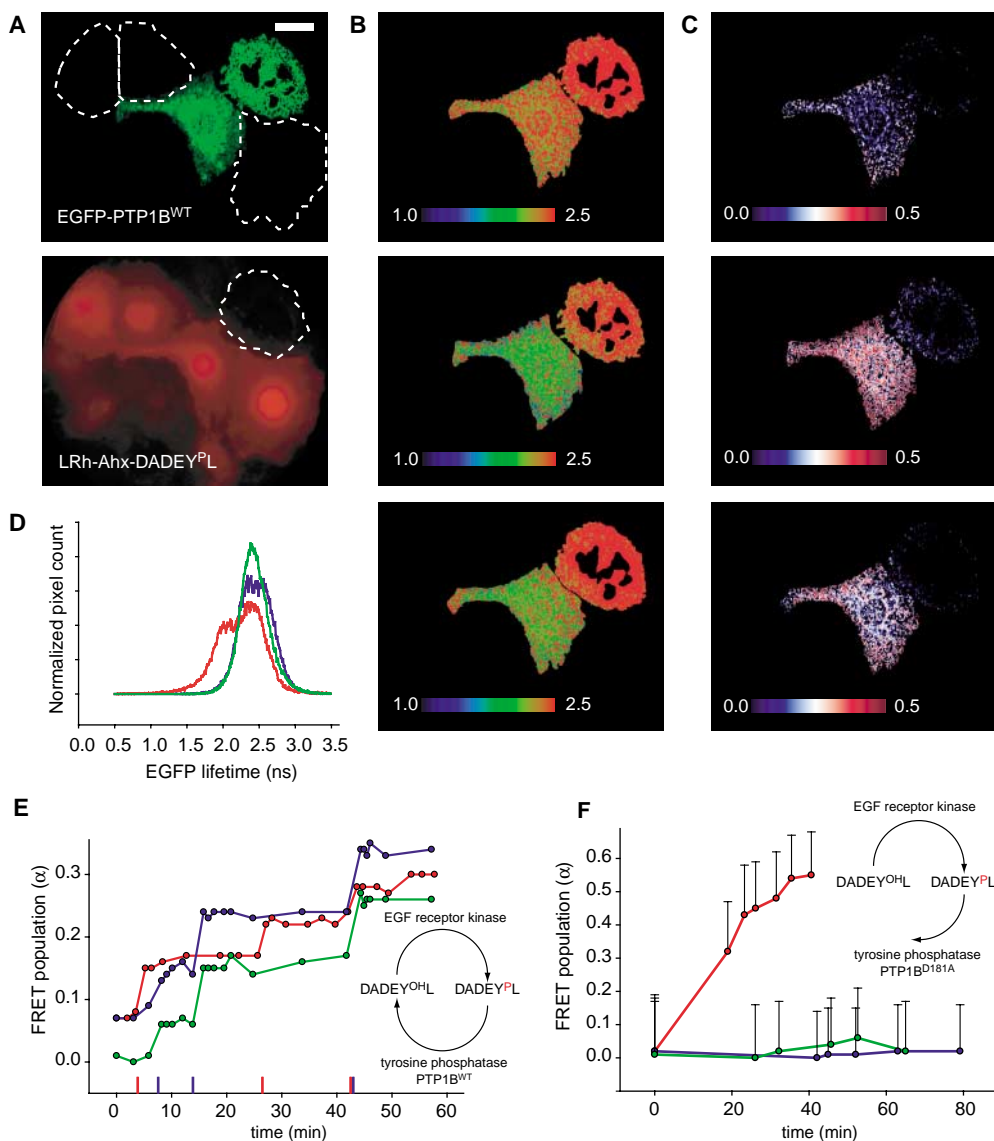
could result from a gradient of phosphorylated peptide and/or differential competitive binding of PTP1B to endogenous substrates. The latter was ruled out by the uniform ES distribution observed in cells transfected with citrine-PTP1B<sup>D181A</sup> (Fig. 3, A to C), which binds the synthetic substrate reversibly and competitively (Fig. 1D and fig. S5).

Systems with spatially partitioned activities—e.g., a plasma membrane-bound kinase and a uniform ER-bound phosphatase (fig. S11)—are expected to generate steady-state substrate concentration gradients (24, 25). In order to explore the contribution of a substrate gradient to the steady-state spatial distribution of an ES complex, we formulated a reaction-diffusion model of the proposed kinase-phosphatase reaction cycle (11). Our model, assuming the in vitro measured kinetic parameters, indeed generated a precipitous gradient (25) of the phosphorylated substrate close to the plasma membrane and also a gradient in ES complex (Fig. 4B). However, the maximal steady-state level of the ES complex predicted by the

reaction-diffusion model was much lower than that observed experimentally (Fig. 3). Instead, the observed ES gradient could only be generated by the model if the specific activity ( $k_{cat}$ ) of the phosphatase was <1% of that in vitro and/or a correspondingly small fraction (<1%) of PTP1B was fully active, consistent with our inference from the slow equilibration time scale shown in Fig. 2C. However, both solutions (the former shown in Fig. 4, A and B) display high sensitivity to relative levels of the kinase, the phosphatase, and the substrate (Fig. 4, A and B, and figs. S12 to S14) (11). This is incompatible with the persistence of the ES gradient to the observed variability of concentrations from cell to cell and implies an additional buffering mechanism in addition to reaction and diffusion.

Such a buffering mechanism could be provided by spatial regulation of the catalytic activity of PTP1B, which can well account for the observed robustness of the ES gradient over a large range of parameters (Fig. 4, C and D)

**Fig. 2.** Establishment of steady-state by kinase-phosphatase reaction cycle in live cells. **(A)** Reporter substrate LRh-Ahx-DADEY<sup>NVOP</sup>-L-CONH<sub>2</sub> (**1-cP**) (bottom) was microinjected into one of two COS-7 cells transiently expressing EGFP-PTP1B<sup>WT</sup> (top). Scale bar, 50  $\mu$ m. **(B)** EGFP lifetime ( $\tau_{\text{phase}}$ , 1.0 to 2.5 ns) images of EGFP-PTP1B<sup>WT</sup>-expressing cells before (top), 15 s (middle), and 1 min (bottom) after 10-s irradiation with 360-nm UV. **(C)** Corresponding images of ES fraction ( $\alpha$ ) determined from global analysis of lifetime data (16). **(D)** Cumulative histogram of lifetime ( $\tau_{\text{phase}}$ ) values of the noninjected (green) and substrate-injected cell, before (blue) and 1 min after (red) UV-induced photolysis. **(E)** Stepwise 360-nm UV-induced uncaging results in higher steady-state level of the EGFP-PTP1B<sup>WT</sup>-substrate complex in LRh-Ahx-DADEY<sup>NVOP</sup>-L-CONH<sub>2</sub>-injected (peptide **1-cP**) COS-7 cells. Typical traces for three individual cells are shown. On the x axis, 10-s UV flashes are indicated as colored ticks. **(F)** Loading MCF-7 cells, cotransfected with the citrine-PTP1B<sup>D181A</sup> and CFP-tagged EGF receptor, with the membrane-permeable nonphosphorylated substrate LRh-C-AEEAc-DADEY<sup>OH</sup>-L-CONH<sub>2</sub> (**2-OH**) results in accumulation of the PTP1B<sup>D181A</sup>-substrate complex over time (red), not seen with the citrine-PTP1B<sup>D181A</sup> alone (green) or in cells coexpressing the catalytically impaired EGFR kinase mutant, EGFR<sup>V741G</sup>-CFP (blue). Error bars show the SD of individual cell traces ( $n = 5$ ).



(11). Here, the lower activity of the membrane-proximal PTP1B pool puts it into a near-saturation regime, whereas higher activity of the central pool buffers the system to perturbations over a larger range (Fig. 4, C and D, and figs. S15 to S17) (11). Spatial regulation also would explain the persistence of the ES gradient in cells with different shapes, as well as in cells

with nonstimulated EGFR localized to endomembranes (fig. S8). Persistence of the ES gradient was also observed after EGFR activation by EGF, which increases its kinase activity by up to a factor of 5 (13). At early times after stimulation, only a slight change in the gradient was observed (Fig. 3E), consistent with the spatial regulation model. Further increase in the steady-state level of ES complex in the cell interior observed at later times could be explained by the redistribution of activated EGFR after endocytosis.

Spatial regulation of PTP1B is likely important for its role in compartmentalized RTK signaling. In the absence of stimulus, the low activity of membrane-proximal PTP1B is still sufficient to counteract basal EGFR activity and, thereby, to maintain a low level of EGFR phosphorylation on endomembranes. With growth factor stimulation, the low activity of the plasma membrane-proximal PTP1B pool also may permit signaling from phosphorylated EGFR in endosomes. Transport of the ligand-activated EGFR to the perinuclear region (8, 9), where PTP1B activity is higher, would then lead to signal termination. Further studies are required to elucidate the biochemical mechanism underlying the spatial regulation of PTP1B activity. Our method for imaging ES intermediates could be used to study the localization and regulation of potentially any enzymatic activity in live cells, providing quantitative information on enzyme catalysis with high specificity.

References and Notes  
 1. A. Ostman, F. D. Bohmer, *Trends Cell Biol.* **11**, 258 (2001).  
 2. P. Chiarugi, P. Cirri, *Trends Biochem. Sci.* **28**, 509 (2003).  
 3. J. V. Frangioni, P. H. Beahm, V. Shifrin, C. A. Jost, B. G. Neel, *Cell* **68**, 545 (1992).  
 4. T. A. Woodford-Thomas, J. D. Rhodes, J. E. Dixon, *J. Cell Biol.* **117**, 401 (1992).  
 5. A. Bourdeau, N. Dube, M. L. Tremblay, *Curr. Opin. Cell Biol.* **17**, 203 (2005).  
 6. M. Miaczynska, L. Pelkmans, M. Zerial, *Curr. Opin. Cell Biol.* **16**, 400 (2004).  
 7. M. Offtenderinger, V. Georget, A. Girod, P. I. Bastiaens, *J. Biol. Chem.* **279**, 36972 (2004).  
 8. F. G. Haj, P. J. Vermeer, A. Squire, B. G. Neel, P. I. Bastiaens, *Science* **295**, 1708 (2002).  
 9. Y. Romsicki, M. Reece, J. Y. Gauthier, E. Asante-Appiah, B. P. Kennedy, *J. Biol. Chem.* **279**, 12868 (2004).  
 10. N. Boute, S. Boubekour, D. Lacasa, T. Issad, *EMBO Rep.* **4**, 313 (2003).  
 11. Materials and Methods are available as supporting material on Science Online.  
 12. Y. X. Fan, L. Wong, T. B. Deb, G. R. Johnson, *J. Biol. Chem.* **279**, 38143 (2004).  
 13. Z. Y. Zhang, D. Maclean, A. M. Thieme-Seffler, R. W. Roeske, J. E. Dixon, *Anal. Biochem.* **211**, 7 (1993).  
 14. P. J. Vermeer, A. Squire, P. I. Bastiaens, in *Methods in Cellular Imaging*, A. Periasamy, Ed. (published for the American Physiological Society by Oxford Univ. Press, New York, 2001), pp. 273–294.  
 15. F. S. Wouters, P. J. Vermeer, P. I. Bastiaens, *Trends Cell Biol.* **11**, 203 (2001).  
 16. P. J. Vermeer, A. Squire, P. I. Bastiaens, *Biophys. J.* **78**, 2127 (2000).  
 17. A. J. Flint, T. Tiganis, D. Barford, N. K. Tonks, *Proc. Natl. Acad. Sci. U.S.A.* **94**, 1680 (1997).  
 18. Single-letter abbreviations for the amino acid residues are as follows: A, Ala; C, Cys; D, Asp; E, Glu; F, Phe; G, Gly; H, His; I, Ile; K, Lys; L, Leu; M, Met; N, Asn; P, Pro;

with nonstimulated EGFR localized to endomembranes (fig. S8). Persistence of the ES gradient was also observed after EGFR activation by EGF, which increases its kinase activity by up to a factor of 5 (13). At early times after stimulation, only a slight change in the gradient was observed (Fig. 3E), consistent with the spatial regulation model. Further increase in the steady-state level of ES complex in the cell interior observed at later times could be explained by the redistribution of activated EGFR after endocytosis.

Spatial regulation of PTP1B is likely important for its role in compartmentalized RTK signaling. In the absence of stimulus, the low activity of membrane-proximal PTP1B is still sufficient to counteract basal EGFR activity and, thereby, to maintain a low level of EGFR phosphorylation on endomembranes. With growth factor stimulation, the low activity of the plasma membrane-proximal PTP1B pool also may permit signaling from phosphorylated EGFR in endosomes. Transport of the ligand-activated EGFR to the perinuclear region (8, 9), where PTP1B activity is higher, would then lead to signal termination. Further studies are required to elucidate the biochemical mechanism underlying the spatial regulation of PTP1B activity. Our method for imaging ES intermediates could be used to study the localization and regulation of potentially any enzymatic activity in live cells, providing quantitative information on enzyme catalysis with high specificity.

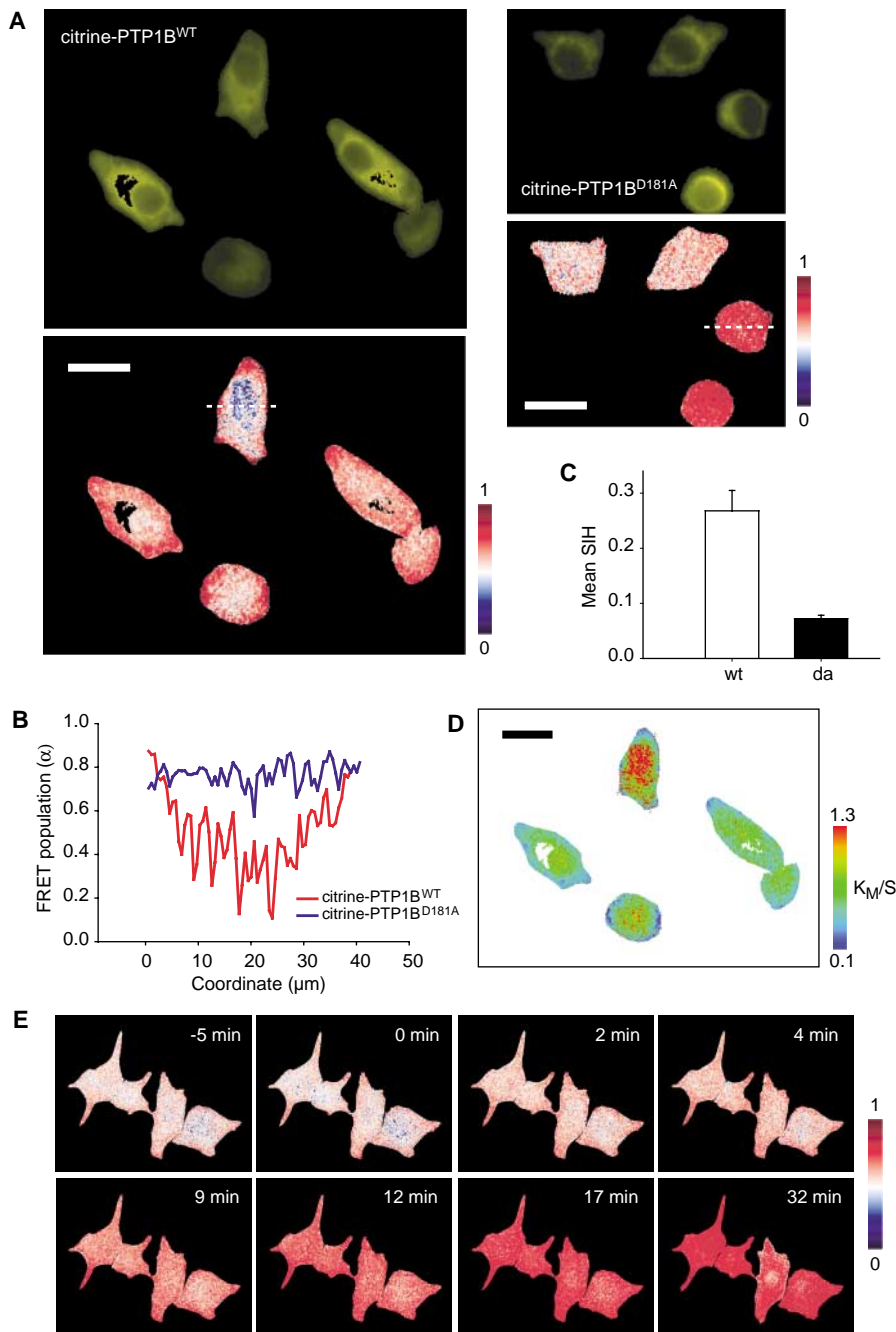


**Fig. 3.** Differential regulation of PTP1B activity in subcellular compartments. **(A)** Images of fraction ( $\alpha$ ) at steady state of ES complex over total citrine-PTP1B<sup>WT</sup> (left) and citrine-PTP1B<sup>D181A</sup> (right) in MCF-7 cells, coexpressing EGFR<sup>WT</sup>-CFP and loaded with the membrane-permeable substrate LRH-C-AEEAc-DADEY<sup>P</sup>L-CONH<sub>2</sub> (2-cP) linked to the penetratin peptide. (top) Fluorescence distribution of citrine-PTP1B. **(B)** Profile of fraction ( $\alpha$ ) across cells in (A) (dashed lines). **(C)** Statistical evaluation of the data in (A). The spatial inhomogeneity (SIH) score is calculated as described in (27). The error bars show SEM of SIH scored in 46 individual cells expressing citrine-PTP1B<sup>WT</sup> (wt) and 47 cells expressing citrine-PTP1B<sup>D181A</sup> (da) in at least four independent experiments. **(D)** Map of  $K_M/S$  for PTP1B<sup>WT</sup>, calculated using Eq. 1. **(E)** Response of ES/E<sub>0</sub> after stimulation with 100 ng/ml EGF at 0 min in MCF-7 cells coexpressing citrine-PTP1B<sup>WT</sup>/EGFR<sup>WT</sup>-CFP and loaded with the membrane-permeable substrate 2-cP linked to penetratin. Scale bars, 50  $\mu$ m.

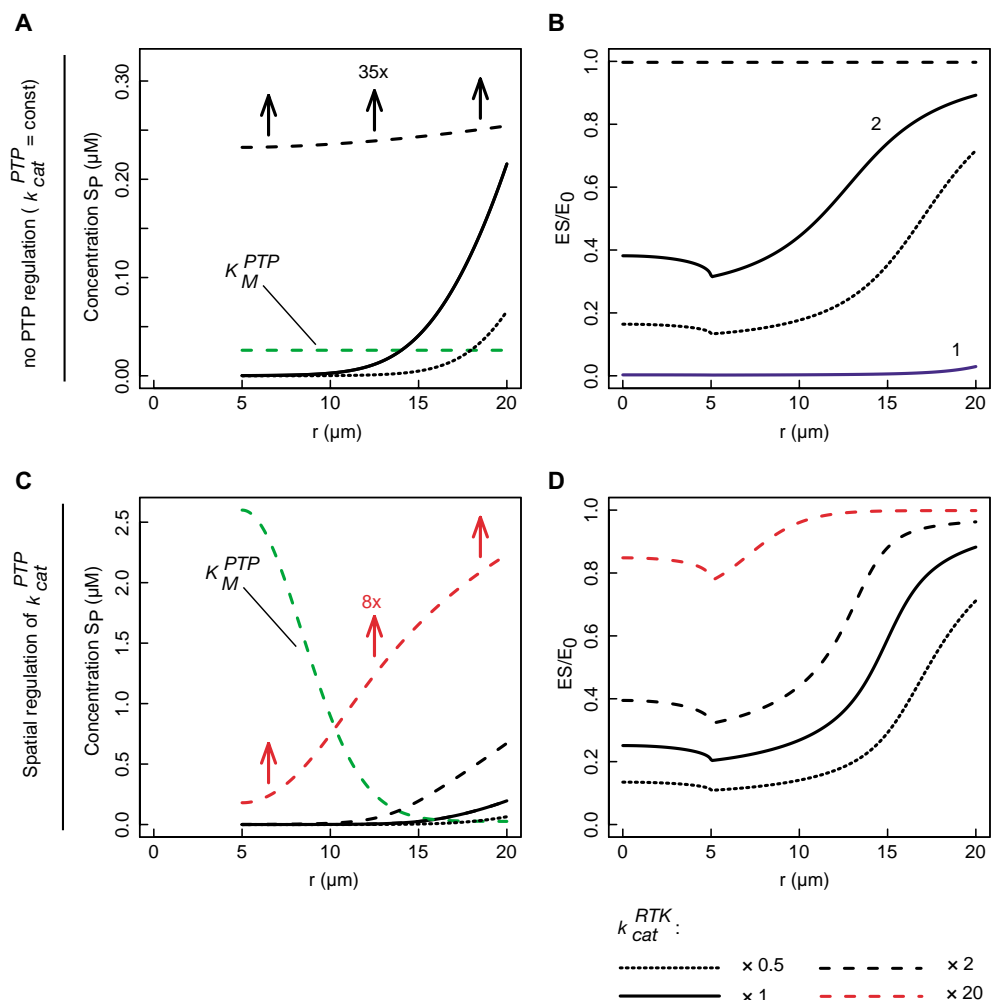


**Fig. 4.** Spherical reaction-diffusion models. **(A)** Phosphorylated substrate concentration (solid line) for a pure reaction-diffusion model using the values given in (11). The cytoplasm extends from the nucleus at 5  $\mu\text{m}$  to the plasma membrane at 20  $\mu\text{m}$ . All values are from observed or in vitro measurements, except for the phosphatase  $k_{cat}^{PTP}$  and  $K_M^{PTP}$  (dashed green line), which were both reduced by a factor of 100. The effect of a factor-of-2 increase (upper dashed curve, divided by 35) and decrease (lower dashed curve) in the kinase  $k_{cat}^{RTK}$  is also shown. **(B)** Two-dimensional projection of the  $ES/E_0$  gradient for the corresponding curves in (A). Also shown is  $ES/E_0$  assuming the in vitro values for all kinetic constants (curve 1). **(C)** Phosphorylated substrate concentration (solid line) for a reaction-diffusion model with additional catalytic regulation of  $k_{cat}^{PTP}$  and  $K_M^{PTP}$  (dashed green line) modeled as a Gaussian curve. At the plasma membrane,  $k_{cat}^{PTP}$  and  $K_M^{PTP}$  are lower than in vitro by 100; at the nuclear radius,  $k_{cat}^{PTP}$  and  $K_M^{PTP}$  assume their in vitro values. A factor-of-2 increase or decrease of the kinase  $k_{cat}^{RTK}$  is also shown (upper and lower dashed curves, respectively). Additionally, a factor-of-20 increase of the kinase  $k_{cat}^{RTK}$  is given (dashed red line, divided by 8). **(D)** Two-dimensional projection of  $ES/E_0$  for the corresponding curves in (C).

Q, Gln; R, Arg; S, Ser; T, Thr; V, Val; W, Trp; X, any amino acid; and Y, Tyr.

19. G. Huyer *et al.*, *J. Biol. Chem.* **272**, 843 (1997).

20. Z. Y. Zhang *et al.*, *Proc. Natl. Acad. Sci. U.S.A.* **90**, 4446 (1993).

21. A. Sawano, S. Takayama, M. Matsuda, A. Miyawaki, *Dev. Cell* **3**, 245 (2002).

22. M. E. Vazquez, M. Nitz, J. Stehn, M. B. Yaffe, B. Imperiali, *J. Am. Chem. Soc.* **125**, 10150 (2003).

23. L. Guo *et al.*, *J. Am. Soc. Mass Spectrom.* **14**, 1022 (2003).

24. G. C. Brown, B. N. Kholodenko, *FEBS Lett.* **457**, 452 (1999).

25. B. N. Kholodenko, G. C. Brown, J. B. Hoek, *Biochem. J.* **350**, 901 (2000).

26. A. Nguyen, D. M. Rothman, J. Stehn, B. Imperiali, M. B. Yaffe, *Nat. Biotechnol.* **22**, 993 (2004).

27. P. Niethammer, P. I. Bastiaens, E. Karsenti, *Science* **303**, 1862 (2004).

28. The authors thank P. Verveer for the estimation of PTP1B kinetic parameters from fitting ES kinetics in vitro, E. Chuntharpursat and F. Haj for help with the experiments, and the anonymous *Science* referees for valuable suggestions. I.A.Y. was supported by Louis Jeantet Fondation de Médecine. The project was partially

supported by grants R01 DK60838 and R37 49152 to B.G.N. and the European Union (LSHG-CT-2003-503259 to C.S. and LSHG-CT-2003-505520 to P.I.H.B.).

**Supporting Online Material**  
[www.sciencemag.org/cgi/content/full/315/5808/115/DC1](http://www.sciencemag.org/cgi/content/full/315/5808/115/DC1)  
 Materials and Methods  
 SOM Text  
 Figs. S1 to S17  
 References

11 September 2006; accepted 21 November 2006  
 10.1126/science.1134966